Eur Spine J (2006) 15: 457–464
DOI 10.1007/s00586-005-0923-5

ORIGINAL ARTICLE

Antonius Rohlmann
Michael Richter
Thomas Zander
Constantin Klöckner
Georg Bergmann

Effect of different surgical strategies on screw forces after correction of scoliosis with a VDS implant

Received: 29 July 2004
Revised: 13 January 2005
Accepted: 28 February 2005
Published online: 24 May 2005

A. Rohlmann (✉) · M. Richter
T. Zander · G. Bergmann
Biomechanics Laboratory,
Charité– Universitätsmedizin Berlin,
Campus Benjamin Franklin,
Hindenburgdamm 30, 12203 Berlin,
Germany
E-mail: rohlmann@biomechanik.de
Tel.: +49-30-84454732
Fax: +49-30-84454729

C. Klöckner
Department of Orthopedics
and Orthopedic Surgery,
Friedrich Alexander University,
Erlangen, Germany

Abstract Pullout of the cranial end-vertebra screw following the correction of a scoliosis with the VDS implant is a common complication. Very little is known about the forces acting on the screws during ventral derotation spondylodesis (VDS) in ventral scoliosis surgery. These forces determine the risk of screw-loosening. The purpose of this study was to identify implant properties and to determine surgical correction strategies that reduce the risk of cranial end-vertebra screw pullout. For this aim, a three-dimensional nonlinear finite element model of a scoliotic thoracic spine was created with a Cobb angle of 61° and 32° rotation. The VDS implant was inserted between T5 and T9. The longitudinal rod diameter, the implant material and seven surgical correction strategies were examined to determine their influence on the Cobb angle as well as on derotation and on axial and transverse forces in the screws. A stiffer implant achieves a better correction but causes higher axial and transverse screw forces. Axial tensile forces act on the screws fixed to the cranial end vertebra and the middle vertebra, while axial compressive forces act on the other screws. A strong correction at the cranial segment leads to high axial and transverse screw forces in the farthest cranial screw and thus to a high risk of screw pullout. The resultant transverse force is often much higher than the axial force component. Simulation of local trunk muscle forces has only a minor effect on the results. The axial tensile forces and thus the risk of screw pullout are highest at the cranial end vertebra. A strategy in which surgical correction is strong in the middle segments and moderate in the outer ones leads to a good reduction of the Cobb angle, a wide derotation angle, and relatively low axial tensile forces at the cranial end vertebra screw.

Keywords Scoliosis · Ventral derotation spondylodesis (VDS) · Finite element analysis · Surgical strategy · Screw force

Introduction

Surgical correction may be indicated for scoliotic thoracic spines with a Cobb angle of more than 40° [4]. Ventral derotation spondylodesis (VDS) is still regarded as one of the most important procedures in ventral scoliosis surgery. It corrects by compression and derotation and achieves excellent surgical results with a short fusion length [3]. The VDS implant (Ulrich Co., Ulm, Germany) is a flexible single-rod system for ventral surgical treatment of scoliosis that was introduced by Zielke et al. [15]. During surgery via an anterior approach, screws are inserted laterally on the convex side of the vertebral bodies. A flexible threaded longitudinal rod is fixed to the screw heads by special nuts whose cylindrical part fits into them. Tightening the two nuts

on either side of the screw head ensures that the rod direction in the head is perpendicular to the screw axis. Correction of scoliosis is achieved by reducing the distances between the screw heads. This means that the nuts on the rod are tightened in the direction of the apical vertebra. The spine is compressed on the convex side and decompressed on the concave side. Segmental derotation requires resection of the intervertebral discs in the bridged region. They can be replaced by bone from the bone mill or bone grafts from the ribs or iliac crest or by cages. The application of bone material or cages depends on the sagittal profile. The outer nut of a screw carries the force component perpendicular to the screw axis, while the nut closer to the apical vertebra mainly serves to secure the rod in the screw head. Little is known about the loads acting in the screws during correction of scoliosis.

On the outermost screws of the VDS implant, a unilateral force acts in the direction of the longitudinal rod, while the other screws are subject to two forces acting in opposite directions, thus reducing the resultant transverse force on the screw. Straightening the spine increases the axial and transverse forces on the screw head. The transverse force may weaken the bone around the thread and lower the pullout resistance against the axial force. Due to the unilateral transverse force acting on the screws, the reduction of pullout strength is most pronounced at the end vertebrae. The width of vertebrae in the frontal plane decreases from caudal to cranial. Thus the cranial end vertebra probably has the lowest pullout strength. This is also the vertebra where most screw pullouts have been observed during VDS, especially in patients with rigid scoliosis [5, 6]. Pullout of the screw does not necessarily occur during corrective surgery. Applying high corrective forces may reduce the fixation strength intraoperatively to the extent that the screw is already on the verge of being pulled out. The screw may be loosened during slight movements without the patient's controlling force, as when shifting the still intubated patient. This complication may require extension of the fusion length or it reduces the outcome of the correction surgery. Moreover, screw dislocation may also cause injury to thoracic or abdominal organs or vessels.

The axial pullout strength of vertebral screws has been measured in vitro [1]. However, it is reduced in surgical correction of scoliosis, since the screws are additionally loaded perpendicular to their axis. Ogon et al. [8] compared fixation strength of single VDS screws and triangulated double screws. They performed pull-out tests and applied a load perpendicular to the screw axis. The triangulated, double-screw fixation led to a 73% increase in resistance against load perpendicular to the screw axis compared with resistance produced using VDS single-screw instrumentation. The pullout force during surgical correction of scoliosis cannot be measured. However, the finite element method enables an analytical estimation of axial forces on the screw head. It also allows the simulation of different strategies for reducing the axial screw force in the cranial end vertebra.

The aims of this paper were to calculate the loads on the screws as well as the changes in Cobb angle and derotation for (i) different implant properties and (ii) several strategies for scoliosis correction.

Methods

Finite element model

A geometrically simplified three-dimensional nonlinear finite element model was created to represent a scoliotic thoracic spine (T1–T12) (Fig. 1). The computer model consisted of vertebral bodies and intervertebral discs. The geometry was transferred from a patient's X-ray. The scoliotic deformity was located at the four segments between T5 and T9. The model had a Cobb angle of 61° and a rotation of 32° at the apical vertebra T7. Volume elements were used for the cortical and cancellous bone of the vertebrae as well as for the nuclei pulposi and the ground substance of the annuli

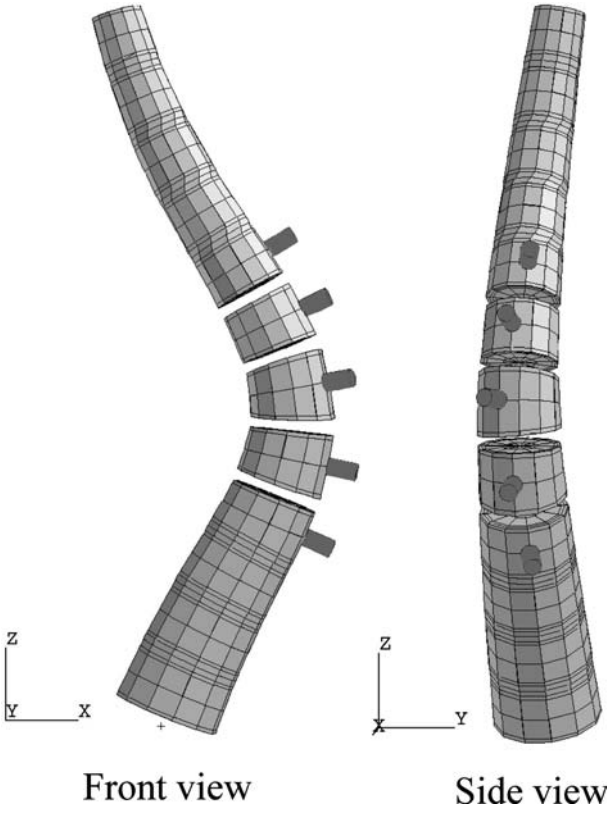

Fig. 1 Element mesh of scoliotic thoracic spine with cylinders indicating screw positions of VDS implant

Table 1 Material properties

Material	Elastic modulus (N/mm^2)	Poisson's ratio (–)
Cortical bone	12,000	0.3
Cancellous bone	500	0.3
Annulus fibrosus	4.2	0.45
Nucleus pulposus	1.1	0.499
Implant steel	210,000	0.3
Titanium alloy	110,000	0.3

fibrosi. The material properties (Table 1) of the different structures were taken from the literature [2, 12–14]. The ligaments, the facet joints and the rib cage were simulated by transverse, axial and rotational spring elements between adjacent vertebrae. The stiffnesses of these spring elements were calculated so that the overall stiffnesses of a segment including the intervertebral disc were the same as those published by Panjabi et al. [9]. The intervertebral discs were removed in the scoliotic region and resection of the rib-heads was assumed at the levels T6–T8. On the one hand, discectomy as well as rib head resection increase the range of motion [7]. On the other hand a scoliotic spine is normally stiffer than a healthy one. Therefore, the respective stiffness values for the spring elements were adapted in an iterative process until the deformations were similar to those found in patients. The intersegmental stiffnesses used in this study lie within the range measured for thoracic functional spinal units [9] and are given in Table 2.

Screws were securely inserted on the convex side of the five vertebrae T5–T9, and a longitudinal rod was connected to the screw heads. The farthest cranial screw is designated as screw 1 and the farthest caudal one as screw 5. The screw positions on the circumference of the vertebral body were chosen according to the axial rotation of the spine. This caused a derotation during the correction procedure. The derotator of the VDS implant was not included in our computer model, since it is not used by many surgeons nowadays. Beam elements were used to represent the screws and rod. In the bridged region, contact was defined as allowing the transmission of compressive force between adjacent vertebrae.

The finite element program ABAQUS and the pre- and post-processor MSC/PATRAN were used. The highly nonlinear model can reproduce large deformities and nonlinear material properties, and contact behavior can be simulated.

Correction of scoliosis

Correction of scoliosis was simulated in two steps. (1) The initially straight longitudinal rod was connected to the screw heads of the scoliotic spine. The rod elasticity exerted different forces on the screw heads and led to a slight correction of the scoliosis. (2) The distance between the end screw heads was reduced by 16 units. The standard case showed a 4-unit reduction in each of the four segments. One unit is equivalent to 1.2 mm.

Implant properties

The VDS implant is available with rod diameters of 3, 4 and 5 mm. If not explicitly stated otherwise, a 3 mm rod was assumed in the model. The VDS implant is normally made of implant steel, but titanium alloy implants are also available. In a parameter study, the rod diameter and elastic material properties were varied accordingly.

Simulated surgical correction strategies

Seven different correction strategies were studied for their effect on the Cobb angle as well as on derotation and screw forces (Table 3). A four-digit number was assigned to each strategy. Rod shortening at the farthest cranial segment T5–T6 is indicated by the first digit, reduction at segment T6–T7 by the second one, and so on. The number 1555, for example, signifies a distance reduction of 1 unit between the screw heads of T5 and T6 and of 5 units between each of the other three segments. The sum of reductions for each strategy was always 16 units.

Table 2 Stiffness coefficients (N/mm for forces and Nm/deg for moments) of a functional spinal unit. The upper part indicates the values used in the current study and the lower part the extreme values calculated from the experimental data of Panjabi et al. [9]

Region	**Forces**			**Moments**				Remark
	Tension	Compression	Shear	Flexion	Extension	Lat.Bending	Axial Rot.	
T1/2-T4/5	770	1,250	110	2.22	2.80	2.80	2.53	Average values from [9]
T5/6-T8/9	770	1,550	235	2.00	2.00	2.18	3.07	
T9/10-T11/12	770	1,250	110	2.22	2.80	2.80	2.53	Average values from [9]
T1/2-T11/12	423	579	41	1.05	1.67	1.73	1.30	Minimum values calculated from [9]
T1/2-T11/12	3,667	11,000	375	3.33	13.3	6.33	5.57	Maximum values calculated from [9]

Table 3 Distance reduction between adjacent screws for different surgical correction strategies

Strategy Code	Reduction at T5/T6 (mm)	Reduction at T6/T7 (mm)	Reduction at T7/T8 (mm)	Reduction at T8/T9 (mm)
1555	1.2	6.0	6.0	6.0
2266	2.4	2.4	7.2	7.2
2662	2.4	7.2	7.2	2.4
4444	4.8	4.8	4.8	4.8
6226	7.2	2.4	2.4	7.2
5551	6.0	6.0	6.0	1.2
6622	7.2	7.2	2.4	2.4

Only a slight distance reduction was achieved at the farthest cranial scoliotic segment by strategies 1555 and 2266 and at the farthest caudal segment by strategies 6622 and 5551 (Table 3). The screw distance reduction was low for both outer segments in strategy 2662 and for the inner segments in strategy 6226. In strategy 4444 the reduction was equal at all segments. Strategy 4444 (with a 3 mm steel rod) is the 'reference case' if not explicitly stated otherwise.

Boundary conditions

The nodal points of the caudal T12 vertebral endplate were rigidly fixed. The patient is anesthetized during surgery and thus exerted no active muscle forces. In a lying position, local muscles stabilize the position of the vertebrae relative to each other when the patient is not anesthetized. These local muscles can be simulated by applying a follower load [10, 11], which is a compressive load whose direction follows the curvature of the spine. In the finite element model the follower load was simulated by forces acting in the centers of the vertebral bodies and directed to the centers of adjacent vertebrae, except for the most cranial vertebra where only a force in the caudal direction was applied. A follower load of 280 N was applied to simulate the situation directly after surgery when the conscious patient is in a lying position.

Evaluation

The following parameters were determined: the Cobb angle, derotation, the axial force at each of the five screw heads, and the resultant force perpendicular to the screw axis acting at the five screw heads.

Results

Effect of implant properties

The Cobb angle is reduced from 61° to 35° by correction with the 3 mm VDS implant and using strategy 4444. With a titanium implant, this angle increases by less than 1°. A 4 mm (5 mm) longitudinal rod reduces the Cobb angle to 31° (25°), thus improving the correction. Derotation is 5.8° for the standard implant and 5.5° for the titanium one. It is increased to 6.9° by a 4 mm rod and to 8.2° by a 5 mm one.

An axial tensile force is calculated for the farthest cranial screw (screw 1) and for screw 3 except in the

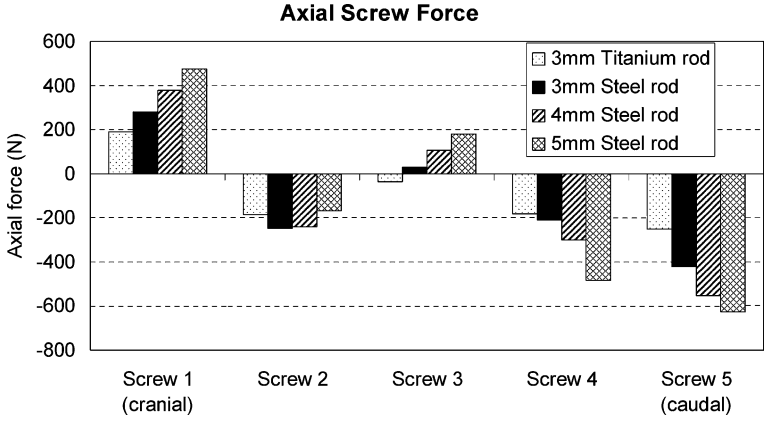

Fig. 2 Axial screw forces for different rod diameters and implant materials. Positive values indicate a tensile force. Standard strategy 4444

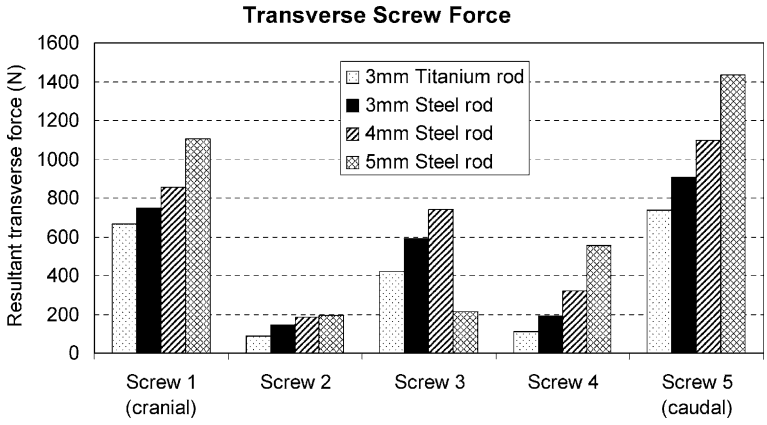

Fig. 3 Transverse screw force for different rod diameters and implant materials. Standard strategy 4444

titanium implant (Fig. 2). Axial compressive forces are predicted for screws 2, 4 and 5. The rod diameter (i.e. its stiffness) has a strong influence on the axial force in the screw head. The axial force increases with the rod diameter, except in screw 2. The lowest axial forces are calculated for the titanium implant. An additional follower load slightly reduces the axial tensile force in screw 1 and increases the tensile force in screw 3, while the follower load has no appreciable effect on the compressive forces in the other screws.

The resultant transverse force is highest at the end screws 1 and 5 (Fig. 3). This transverse force increases with the rod diameter except in screw 3, where the 5 mm rod causes a relatively low force. The lowest transverse force is normally predicted for the titanium implant. Applying a follower load reduces the maximum transverse force in the outer screws by about 10%. The other transverse loads are similar to those seen in the model without a follower load.

Effect of surgical correction strategies

Figure 4 shows the shapes of the corrected thoracic spine for strategies 2266, 4444 and 6622. Bone contact is predicted at the two lower bridged segments for strategy 2266 and at the two upper segments for 6622. No bone contact is found for strategy 4444.

The Cobb angle correction is highest with an only slight correction of the upper bridged segment (Fig. 5). The Cobb angle differs by 6.3° for the various strategies studied.

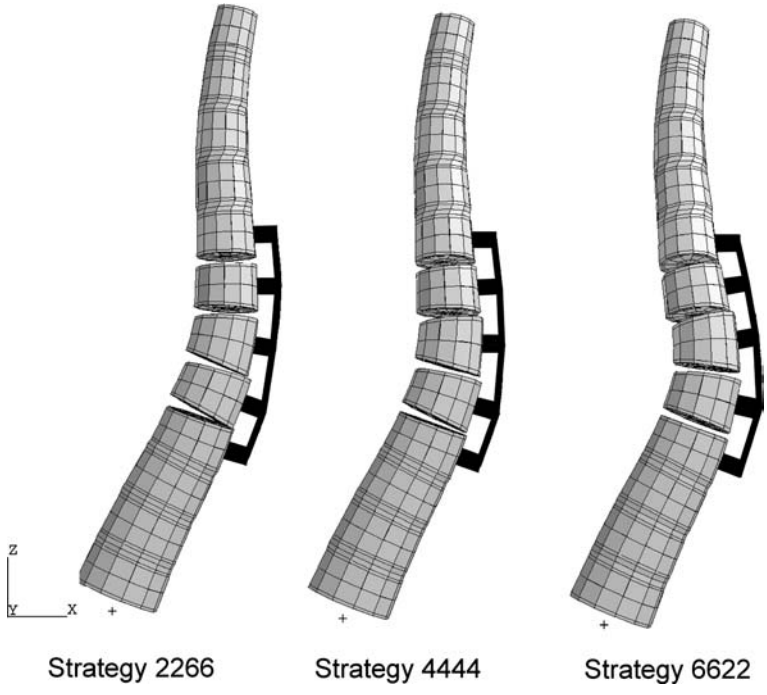

Fig. 4 Shape of thoracic spine after correction by different strategies. Standard 3 mm steel rod. Note the different intervertebral spaces at the level of the implant

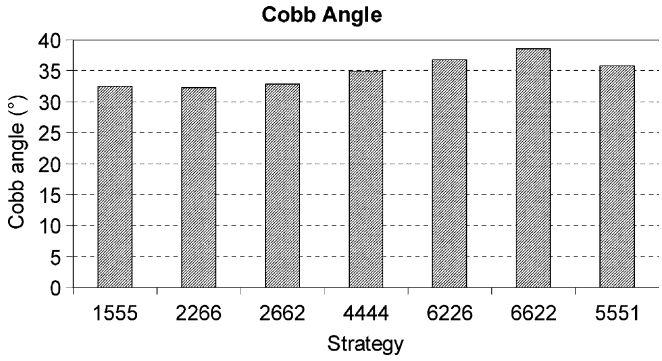

Fig. 5 Calculated Cobb angle for different surgical strategies. Standard 3 mm steel rod

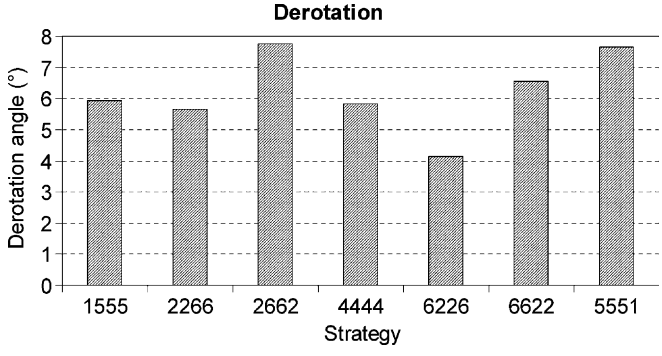

Fig. 6 Calculated derotation angle for different correction strategies. Standard 3 mm steel rod

Derotation is maximum for the correction mainly at the two inner segments (strategy 2662) and minimum for that mainly at the outer ones (strategy 6226) (Fig. 6). The two extreme derotation angles differ by 3.7° in our model.

Axial tensile screw forces are calculated in screw 1 for all strategies (Fig. 7). The axial force in screw 1 is high in conjunction with marked shortening at the upper bridged segments. There are normally compressive forces in screws 2, 4 and 5. High positive forces in screw 3 for strategy 2266 and in screw 4 for strategy 6226 as well as a negative force in screw 3 for strategy 6622 are predicted for strategies where regions of high and low correction meet. This means that the corresponding vertebra comes into bone contact with the adjacent one during correction, and the center of rotation changes accordingly. Applying a follower load leads to the same axial force pattern for the different strategies and screws as in Fig. 7. However, it decreases the tensile force in screw 1 and increases the force in screw 3.

The resultant transverse force at screw 1 is high in conjunction with marked shortening at the upper level (Fig. 8). It is high at screw 5 when the correction at the caudal segment is high. High transverse forces are calculated at screws 2 to 4 for strongly differing corrections in the adjacent segments. The highest transverse forces are calculated for screw 5 and strategies 2266 and 6226. The forces perpendicular to the screw axis are not appreciably influenced by a follower load.

Discussion

A finite element model of the thoracic spine was used to simulate different implant properties and surgical strategies for correction of scoliosis with a VDS implant. This study has a number of limitations. The investigation covered only one type of scoliosis with a Cobb angle of 61° and a rotation of 32°, although each type is different. Only the situations during the surgical procedure and immediately postoperatively were studied since they represent the situations where most screw pullouts occur. Like all finite element studies dealing with the spine, this one also required several assumptions and simplifications. A simplified geometry was applied in representing the vertebrae as cylindrical bodies. Several spring elements in the intervertebral space were used to

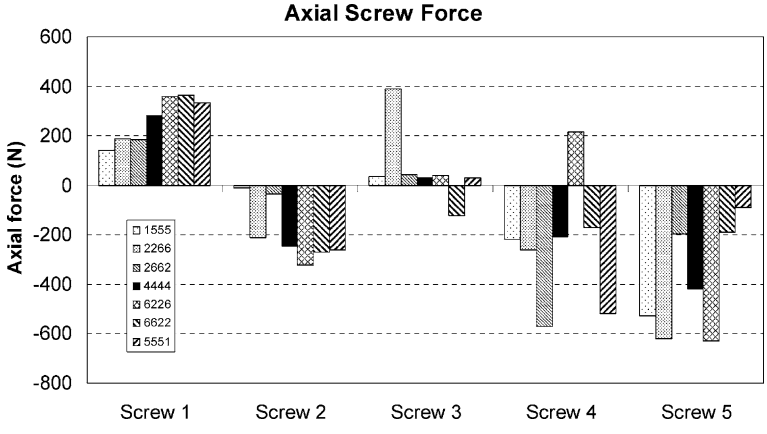

Fig. 7 Comparison of axial screw forces for different correction strategies. Standard 3 mm steel rod

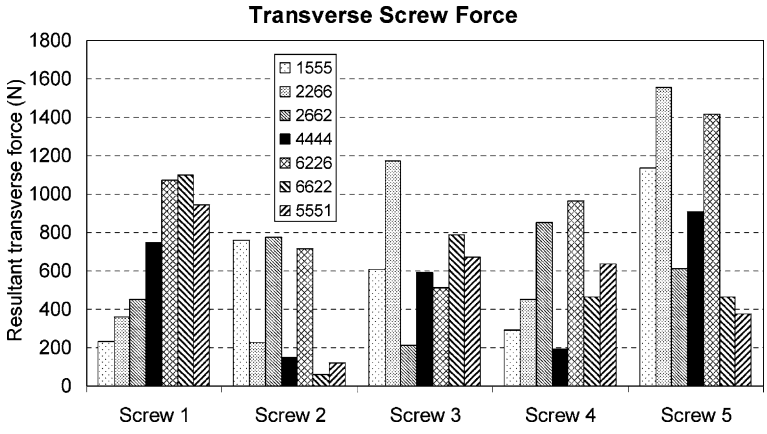

Fig. 8 Comparison of resultant transverse force for different correction strategies in scoliosis surgery. Standard 3 mm steel rod

simulate the posterior parts of the vertebra, the rib-cage and the ligaments. The springs were adapted to intervertebral stiffness values reported in the literature. The material properties of the different spinal structures were also taken from the literature. They were determined in normal specimens and may thus differ from those of a scoliotic spine. Bone grafts or cages were not included in the model since, if at all, they are normally placed anteriorly to avoid an unphysiological spinal curve in the sagittal plane. In addition, they are mostly inserted during the last phase of the correction procedure. However, a stiff bone graft or a cage may alter the center of rotation of a vertebra and thus affect the screw forces. In a pilot study, we could show that bone meal in the intervertebral space has only a minor effect on the results.

The local muscles were represented by a follower load, but it has not yet been proven that this delivers realistic results in the case of a scoliotic spine. Only one value was used for the follower load in this study. Since we were mainly interested in the axial screw forces, the computer model was loaded by the implant and a follower load, while all other forces were disregarded. All these simplifications suggest that the results are qualitative and should be seen as trends rather than exact values.

Finite element models of complex structures like the spine should generally be validated by experimental data. Only very few measured data are available on scoliotic spines since it is extremely difficult to obtain such specimens. To our knowledge, there are no experimental data on implant screw forces during the correction of scoliosis. The scoliotic thoracic spine is curved in the sagittal and frontal planes and rotated in the transverse plane. It is not easy to predict the forces acting on the screws. Therefore a pilot study was done using a model curved only in the frontal plane. After insertion of the implant, the axial screw forces showed the expected pattern, i.e. tensile axial forces in the outer and compressive ones in the inner screws. The load components in the longitudinal rod segments and the loads on the screw part inside the vertebral body were also studied to check the model.

Clinical decisions should not be made solely on the base of finite element calculations since the computer models represent mostly an ideal situation and many factors and possible situations are neglected. This is especially true when the computer model cannot be validated with experimental data. Our results quantitatively justify the intuitive approach of many spine surgeons. Since each scoliosis is different, only trends can be expected from a finite element study.

A stiffer implant (thicker rod) leads to a lower Cobb angle and higher derotation, since the predetermined reduction of screw distances on the threaded rod causes a smaller deformation of the implant itself. Correction mainly in the outer segments (strategy 6226) slightly improves the Cobb angle and the derotation. The best correction of the Cobb angle is achieved with a thick longitudinal rod and a small correction at the cranial segment. The greatest derotation is achieved by a thick implant rod and a small correction at the caudal segment. Our model did not assume the application of the derotator. Instead, the screws were placed according to the rotation of the spine. During surgery, the distances between screw heads are not reduced in one step but in intervals to allow relaxation of the soft tissues. Our computer model did not account for the viscoelastic behavior of the spine.

During correction, bone contact is established between adjacent vertebrae by their gradual convergence. The point of contact then becomes the center of rotation for further correction. There is also a strong increase in the stiffness and screw forces. This explains the high screw forces associated with certain strategies (Figs. 7 and 8). When stiff bone grafts or cages are inserted in the intervertebral space prior to correction they may become the center of rotation, which may affect the screw forces and the correction angle. The results will then depend on the level of the stiff bone graft or cage and the position within the intervertebral space.

An axial tensile force is found in the screw of the cranial end vertebra and in screw 3. The axial force in the latter is normally much smaller than in screw 1. The axial compressive force in the other screws does not cause screw pullout. In the screw of the cranial end vertebra, the axial tensile force is highest for a stiff longitudinal rod. A strong correction at the farthest cranial segment also increases the axial tensile force in screw 1. Low axial tensile forces in screw 1 are achieved by a 3 mm titanium rod and small corrections at the farthest cranial segment.

The resultant force perpendicular to the screw axis is highest at the screws of the end vertebrae (screws 1 and 5) in cases with a uniform correction at all segments (Fig. 3). In the other screws, the caudally directed transverse correction force partly compensates the cranially directed one. The relatively high transverse force at screw 3 is partly due to the force causing the derotation. Rotation is greatest at the apical vertebra. A high transverse force reduces the pullout strength of a screw and may even cause the screw to cut through the cancellous bone of the vertebral body. Screw 1 has a low transverse force if the correction at the farthest cranial segment is small.

A high transverse force widens the screw hole due to the viscoelastic behavior of bone. Combined with a high axial screw force, this leads to a high risk of screw pullout. Strategy 2662 results in a marked reduction of the Cobb angle, a wide derotation angle, a relatively low axial tensile force in screw 1 and moderate transverse forces in the other screws. Thus our calculations predict that this strategy achieves good scoliosis correction with a low risk of screw pullout. It must be noted, however, that the sum of segment corrections is not constant during surgery. Thus combinations other than the one studied may lead to slightly better results.

Conclusions

The axial tensile forces and thus the risk of screw pullout are highest at the cranial end vertebra. A stiffer implant achieves a better correction but causes higher axial and transverse screw forces. A strategy in which surgical correction is strong in the middle segments and moderate in the outer ones leads to a good reduction of the Cobb angle, a wide derotation angle, and relatively low axial tensile forces at the cranial end vertebra screw.

Acknowledgements Finite element analyses were performed at the Norddeutscher Verbund für Hoch- und Höchstleistungsrechnen (HLRN) and the Zentraleinrichtung Rechenzentrum Berlin (ZRZ). The authors thank Dr. J.Weirowski for editorial assistance.

References

1. Eysel P, Schwitalle M, Oberstein A, Rompe JD, Hopf C, Kullmer K (1998) Preoperative estimation of screw fixation strength in vertebral bodies. Spine 23:174–180
2. Goel VK, Monroe BT, Gilbertson LG, Brinckmann P (1995) Interlaminar shear stresses and laminae separation in a disc. Finite element analysis of the L3-L4 motion segment subjected to axial compressive loads. Spine 20:689–698
3. Halm H (2000) Ventrale und dorsale korrigierende und stabilisierende Verfahren bei idiopathischer Skoliose. Orthopäde 29:543–562
4. Hopf C (2000) Kriterien zur Behandlung idiopathischer Skoliosen zwischen 40° und 50°. Operative vs. konservative Therapie. Orthopäde 29:500–506
5. Klöckner C, Walter G, Matussek J, Weber U (2000) Ventrodorsale Korrektur und Instrumentation idiopathischer Skoliosen. Orthopäde 29:571–577
6. Moe J, Purcell G, Bradford D (1983) Zielke Instrumentation (VDS) for the Correction of Spinal Curvature. Clin Orthop 180:133–153
7. Oda I, Abumi K, Cunningham BW, Kaneda K, McAfee PC (2002) An in vitro human cadaveric study investigating the biomechanical properties of the thoracic spine. Spine 27:E64–E70
8. Ogon M, Haid C, Krismer M, Sterzinger W, Bauer R (1996) Comparison between single-screw and triangulated, double-screw fixation in anterior spine surgery. A biomechanical test. Spine 21:2728–2734
9. Panjabi MM, Brand RA, White III AA (1976) Mechanical Properties of the Human Thoracic Spine. J Bone Joint Surg Am 58-A:642–652
10. Patwardhan AG, Havey RM, Meade KP, Lee B, Dunlap B (1999) A follower load increases the load-carrying capacity of the lumbar spine in compression. Spine 24:1003–1009
11. Rohlmann A, Neller S, Claes L, Bergmann G, Wilke H-J (2001) Influence of a follower load on intradiscal pressure and intersegmental rotation of the lumbar spine. Spine 26:E557–E561
12. Rohlmann A, Zander T, Bergmann G (2005) Effect of total disc replacement with ProDisc on the biomechanical behavior of the lumbar spine. Spine 30(7):738–743
13. Shirazi-Adl A, Ahmed AM, Shrivastava SC (1986) Mechanical response of a lumbar motion segment in axial torque alone and combined with compression. Spine 11:914–927
14. Zander T, Rohlmann A, Calisse J, Bergmann G (2001) Estimation of muscle forces in the lumbar spine during upper-body inclination. Clin Biomech 16:S73–S80
15. Zielke K, Stunkat R, Duquesne J, Beaujean F (1975) Ventrale Derotationsspondylodese. Orthopädische Praxis 11:562–569